Zhang *et al.*
European Journal of Medical Research (2025) 30:162
https://doi.org/10.1186/s40001-025-02416-7

European Journal of Medical Research

RESEARCH

Open Access

Vagus nerve stimulation alleviates myocardial injury following hepatic ischemia–reperfusion in rats by inhibiting ferroptosis via the activation of the SLC7A11/GPX4 axis

Po Zhang[1†], Yuanjing Qin[1†], Haiyan Wang[1] and Jinping Wang[2*]

Abstract

Background Vagus nerve stimulation (VNS) exhibits protective effects against remote organ injury following ischemia–reperfusion (I/R). However, its effects on acute myocardial injury induced by hepatic I/R in rats, and the underlying mechanisms, remain unclear.

Methods Thirty male rats were randomly assigned to five groups: Sham, I/R, VNS, VNS + Erastin, and VNS + DMSO. A hepatic I/R injury model was established by occluding the arterial and portal veins of the left and middle lobes of the liver for 1 h followed by 6 h of reperfusion. VNS was performed throughout the hepatic I/R process. Erastin was administered intraperitoneally 60 min before hepatic ischemia. Blood samples were collected from the left common carotid artery post-reperfusion to measure liver injury markers (alanine aminotransferase [ALT] and aspartate aminotransferase [AST]) and the myocardial injury marker (cardiac troponin I [cTnI]). Left ventricular myocardial tissue was also collected for ultrastructural analysis via transmission electron microscopy, reactive oxygen species (ROS) detection using dihydroethidium staining, and measurements of Fe^{2+} levels, malondialdehyde (MDA) concentration, glutathione (GSH) levels, and superoxide dismutase (SOD) activity. Western blotting assessed the expression of ferroptosis-related proteins SLC7A11 and GPX4 in the myocardial tissue.

Results VNS significantly reduced serum levels of ALT, AST, and cTnI, while also mitigating mitochondrial damage in cardiomyocytes. Additionally, VNS decreased ROS levels, alleviated iron overload, and reduced lipid peroxidation in myocardial tissue. These protective effects were associated with the activation of the SLC7A11/GPX4 axis, as evidenced by increased expression of these proteins in the VNS group. However, the cardioprotective effects of VNS were negated by the ferroptosis activator erastin, indicating that ferroptosis is involved in VNS-mediated cardioprotection.

Conclusion VNS protects against myocardial injury from hepatic ischemia–reperfusion, likely by inhibiting oxidative stress and ferroptosis through activation of the SLC7A11/GPX4 axis.

Keywords Myocardial injury, Hepatic ischemia/reperfusion injury, Ferroptosis, Vagus nerve stimulation

[†]Po Zhang and Yuanjing Qin have contributed equally to the work.

*Correspondence:
Jinping Wang
jcdyywangjinping@163.com
Full list of author information is available at the end of the article

Background

Hepatic ischemia–reperfusion injury is a common complication during liver resection, liver transplantation, and hemorrhagic shock, significantly contributing to postoperative morbidity and mortality [1, 2]. HIRI not only severely impairs liver function but can also cause remote organ injury, including lungs, kidneys, intestines, pancreas, brain, and heart, potentially resulting in multiple organ failure [3, 4]. Under normal physiological conditions, the body uses its endogenous antioxidant system to eliminate the continuously produced free radicals and reactive oxygen species (ROS), thereby maintaining redox dynamic physiological balance, but ischemia can disrupt this balance [5]. The heart, as the first organ to receive blood flow post-HIR, is highly vulnerable to attacks by ROS, which can cause myocardial injury and severely affects the patient's prognosis [5, 6]. Furthermore, during ischemia–reperfusion, excessive activation of the sympathetic nervous system leads to autonomic nervous system imbalance [7], increased cardiac oxygen consumption, and oxygen supply–demand imbalance, further exacerbating myocardial damage. Therefore, exploring effective treatments and their mechanisms to mitigate myocardial injury caused by HIRI is of great significance for improving patient prognosis.

Recent studies have highlighted ferroptosis, a novel form of non-apoptotic cell death, as a significant factor in cardiovascular diseases [8, 9]. This process is characterized by iron overload, elevated production of ROS, and lipid peroxidation, all of which contribute to cardiomyocyte injury [9]. Specifically, excess iron within the cell, particularly the highly reactive ferrous ions, initiates lipid peroxidation through the Fenton reaction, catalyzing the peroxidation of polyunsaturated fatty acids (PUFAs) highly expressed on the cell membrane [10].The peroxidation product PUFA-OOH generated during this process has strong cytotoxicity, which can damage the cell membrane structure, increase membrane permeability, thereby accelerating the ferroptosis process and leading to myocardial injury [11]. Key regulators of this process include glutathione peroxidase-4 (GPX4) and the cystine-glutamate antiporter system (xCT), which consists of SLC7A11 and SLC3A2 subunits. Among them, the SLC7A11 subunit transports extracellular cysteine into the cell, providing sufficient substrate for GSH synthesis, while the SLC3A2 subunit serves as a molecular chaperone for SLC7A11, ensuring its proper localization on the cell membrane [11]. Inhibition of SLC7A11 or reduction of GPX4 activity can exacerbate lipid peroxidation, thereby triggering ferroptosis and leading to myocardial injury [12].

Vagus nerve stimulation (VNS) has been widely used in the treatment of various diseases, including refractory epilepsy, depression, obesity, and stroke rehabilitation [13–15]. Moreover, VNS has also shown significant effects in alleviating ischemia–reperfusion (I/R) injury in organs such as the kidneys, brain, liver, and heart, as well as the remote organ damage it induces [16–22]. Notably, VNS effectively reduces myocardial I/R injury and promotes myocardial function recovery by activating cholinergic anti-inflammatory pathways, antioxidant stress, and anti-apoptotic mechanisms, highlighting its potential in cardiac protection [23–25]. However, the molecular mechanisms of VNS-mediated cardiac protection have not yet been fully elucidated, particularly whether it achieves cardioprotection through the regulation of the SLC7A11/GPX4 ferroptosis pathway remains to be studied. Therefore, this study aims to investigate the protective effect of VNS on myocardial injury after hepatic I/R injury in rats and to further analyze whether this is achieved through the regulation of the SLC7A11/GPX4 ferroptosis pathway. Through the study, we hope to provide new theoretical basis and experimental support for the application of VNS in the field of cardiac protection, and to offer new ideas for myocardial protection strategies in clinical liver surgery and transplantation.

Materials and methods

Animals and experimental protocol

Healthy male Sprague–Dawley rats, aged 6–8 weeks and weighing between 250–280 g, were obtained from the Experimental Animal Center of Shanxi Medical University. They were housed in a controlled environment with a 12 h light/dark cycle at (23 ± 2) ℃, and had unrestricted access to animal chow and water. They were allowed to acclimate to the laboratory environment for one week prior to the experiments. This study was approved by the Ethics Committee of the Second Hospital of Shanxi Medical University (DW2024028), adhering to the guidelines outlined in the Guide for the Care and Use of Laboratory Animals by the National Institutes of Health. All experiments were conducted at the main campus of the Second Hospital of Shanxi Medical University, with efforts made to minimize the number of animals used and their suffering.

Thirty rats were randomized into five groups: Sham group (Sham, $n=6$), I/R group (Hepatic ischemia–reperfusion injury, $n=6$), VNS group (Vagus nerve stimulation + hepatic ischemia–reperfusion injury, $n=6$), VNS + Erastin group (Vagus nerve stimulation + hepatic ischemia–reperfusion injury + Erastin, $n=6$), and VNS + DMSO group (Vagus nerve stimulation + hepatic ischemia–reperfusion injury + DMSO, $n=6$). In the Sham group, the hepatic pedicle of the rats was isolated but not clamped, while the rats in the other groups underwent hepatic pedicle clamping for 1 h, followed by reperfusion

for 6 h. In the Sham and I/R groups, the vagus nerve was exposed but not electrically stimulated, while the remaining groups of rats received continuous VNS throughout the entire I/R process. In the VNS + Erastin group, erastin (S7242, Selleck, USA) 14 mg/kg dissolved in 1% DMSO was injected intraperitoneally 1 h before ischemia [26]. In the VNS + DMSO group, 1% DMSO (as the solvent control for erastin) was injected intraperitoneally 1 h before ischemia. The experimental design is shown in Fig. 1.

Preparation of the hepatic ischemia–reperfusion injury model

Following the methodology of Zhang et al. [19], an acute segmental (70%) liver ischemia–reperfusion (I/R) injury model was established in this experiment. Prior to surgery, all rats were fasted overnight. On the day of the surgery, the animals were weighed and anesthetized via intraperitoneal injection of 25% urethane (1.25 g/kg body weight). Local anesthesia was applied at the surgical sites using 0.25% bupivacaine (total volume < 1 ml). Briefly, a midline incision was made in the upper abdomen to expose the peritoneal cavity. Using a microvascular clamp, the portal vein, hepatic artery, and bile duct (i.e., the hepatic pedicle) are clamped from the upper side of the right lobe of the liver. After one hour, the clamp was removed, and the abdominal cavity was sutured, restoring blood flow to the liver for six hours. During both the ischemic and reperfusion periods, a heating pad was used to maintain a constant body temperature in the rats.

Vagus nerve stimulation

Considering that stimulation of the left vagus nerve has a minimal impact on heart rate and cardiac function [27], this study chose the left cervical vagus nerve trunk as the stimulation target. The left vagus nerve was carefully separated from the surrounding connective tissue through a mid-cervical incision. Gently hook the protective electrode onto the left vagus nerve, with the other end connected to a stimulator (Chengdu Instrument Factory, Chengdu, Sichuan, China). During the entire hepatic I/R process, continuous single electrical stimulation was applied at a stimulation frequency of 20 Hz and a pulse width of 0.1 ms. Throughout the experiment, an electrocardiogram (lead II, RM6240, Chengdu Instrument Factory, Sichuan, Chengdu, China) monitored the heart's electrical activity. A catheter was inserted retrogradely through the left common carotid artery and connected to a transducer to continuously record arterial blood pressure and heart rate. Based on the recorded electrocardiogram, adjusted the stimulation intensity to reach a 10% reduction in the sinus rate, and readjusted every hour.

Collection of blood and tissue samples

After reperfusion for 6 h, blood samples were collected from the left general carotid artery and centrifuged at 4200 rad/min for 15 min at 4 °C. Then the serum was extracted and cryopreserved at − 80 °C for further analysis. After euthanasia of the animals via overdose of the anesthetic, myocardial tissues were collected quickly from each rat and divided into three parts: one part is

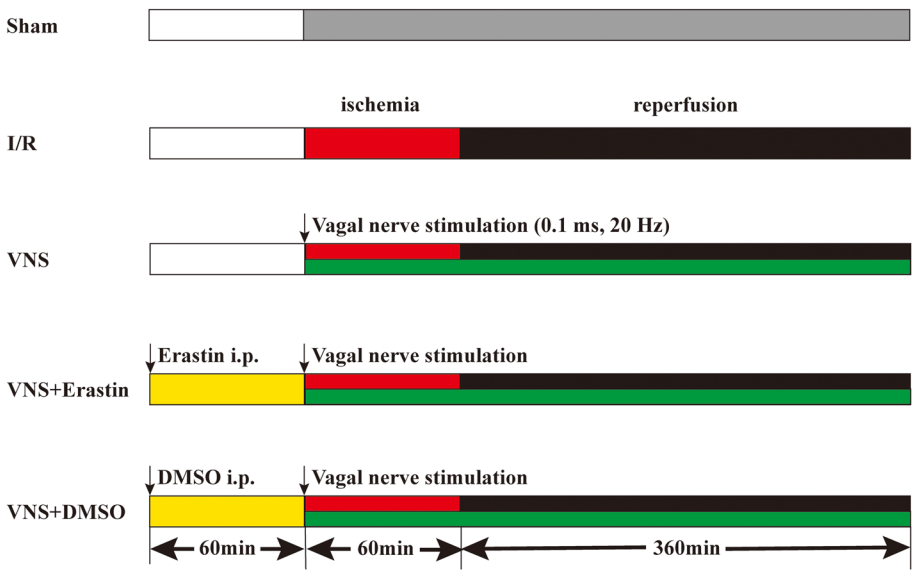

Fig.1 Diagram of the experimental design. The yellow area represents 14 mg/kg erastin administered 60 min before ischemia (i.p.); the red area represents ischemia time; the black area represents reperfusion time; the green area represents the time when vagus nerve stimulation was given

fixed for observing mitochondrial ultrastructure, one part is prepared as frozen sections, and the remaining part is stored at − 80 °C for further evaluation.

Analysis of alanine aminotransferase (ALT), aspartate aminotransferase (AST) and cardiac troponin I (cTnI) in serum levels

To assess liver function, serum ALT and AST levels were measured using specific detection kits (Jiancheng Bioengineering Institute, Wuhan, China). At the same time, enzyme-linked immunosorbent assay kits (Elabscience, Wuhan, China, Cat no. E-EL-R1253c) were used to measure serum levels of the myocardial injury marker cTnI according to the manufacturer's instructions.

Transmission electron microscopy

The samples were fixed in 2.5% glutaraldehyde (PH 7.4) for 2 h. After being washed three times with 0.1 M phosphate buffer (PH 7.2) and fixed in 1% osmic acid at 4 ℃ for 2 h. Then the samples were gradient dehydrated in a graded series of ethanol solutions. Subsequently, the samples were embedded in Epon-Araldite resin for penetration and placed in a mold for polymerization. After the semi-thin section was used for positioning, the ultrathin section was made and collected for microstructure analysis. The sections were counterstained with 3% uranyl acetate and 2.7% lead citrate. Then observed by electron microscope (HT7700, Hitachi, Tokyo, Japan).

Dihydroethidium (DHE) staining

The left ventricular myocardial tissue was obtained and embedded in optimal cutting temperature (OCT) compound, followed by the preparation of 10 μm frozen sections on a freezing microtome (Leica CM 1850, Nussloch, Germany). The sections were outlined with a histochemical pen and incubated with 10 μM dihydroethidium (Beyotime, Shanghai, China) at 37 °C in the dark for 30 min. Subsequently, the sections were washed three times with phosphate-buffered saline (PBS), each wash lasting for 5 min. The samples were then treated with an antifade reagent and mounted under coverslips. Fluorescence images were captured with a fluorescence microscope (Olympus, BX51, Japan), and the fluorescence intensity was semi-quantitatively analyzed utilizing ImageJ software (version 1.48, NIH, USA).

Measurements of oxidative stress and Fe^{2+} content in myocardial tissue

The left ventricular myocardial tissue samples were homogenized. The levels of MDA, GSH, and SOD were measured according to the instructions provided with the respective assay kits (Jiancheng Bioengineering Institute, Nanjing, China). Additionally, Fe^{2+} content was detected using a ferrous ion colorimetric assay kit (Elabscience, Wuhan, China) to evaluate the iron load status of the myocardial tissue.

Western blot analysis

The samples of ventricular myocardium were homogenized in RIPA lysis buffer (Beyotime, Shanghai, China) containing 1% PMSF protease inhibitor (Beyotime, Shanghai, China) to extract total protein. After centrifugation, the supernatant was collected. Protein concentrations were quantified using the BCA protein assay kit (Boster, Wuhan, China). The lysed proteins (20 μg) were separated by 10% SDS polyacrylamide gel (Boster, Wuhan, China) for electrophoresis, then transferred to a polyvinylidene fluoride (PVDF) membrane (Merck Millipore, Germany). Placed the PVDF membrane in a protein-free rapid blocking solution (Boster, Wuhan, China) and blocked at room temperature for 20 min. The membrane was then incubated overnight at 4 °C with primary antibodies specific for GPX4 (Proteintech, Wuhan, China, Cat no. 67763-1-Ig, 1:5000), SLC7A11 (Affinity Biosciences, OH, USA, Cat no. DF12509, 1:1000), and the internal control GAPDH (Elabscience, Wuhan, China, Cat no. E-AB-40337, 1:5000). After washing with Tris-buffered saline containing Tween (TBST), the membrane was incubated with a secondary antibody (Boster, Wuhan, China, Cat no. BA1050, 1:10,000; Elabscience, Wuhan, China, Cat no. E-AB-1003, 1:10,000) at room temperature for 2 h. Then the membrane was washed with TBST. The protein bands were visualized by the chemical luminescence method and photographed using a gel imaging system (Gel DocTM XR Imaging System, Bio-RAD, USA). Finally, semi-quantitative analysis of protein expression was conducted using ImageJ software (version 1.48, NIH, USA) and normalized in comparison with the GAPDH.

Statistical analysis

The experimental data that passed the normality test were expressed as mean ± standard deviation. Statistical analysis and data visualization were performed using GraphPad Prism 9.5. Intergroup differences were evaluated using one-way analysis of variance (ANOVA), followed by Bonferroni's multiple comparison test for post hoc analysis. Statistical significance was set at $P < 0.05$.

Results

The effect of VNS on serum biochemical indicators after hepatic ischemia–reperfusion injury in rats

To evaluate the protective effect of VNS on hepatic I/R and the resulting myocardial injury, we measured serum levels of ALT, AST, and cTnI. At 6 h after reperfusion, serum ALT and AST levels in the I/R group were

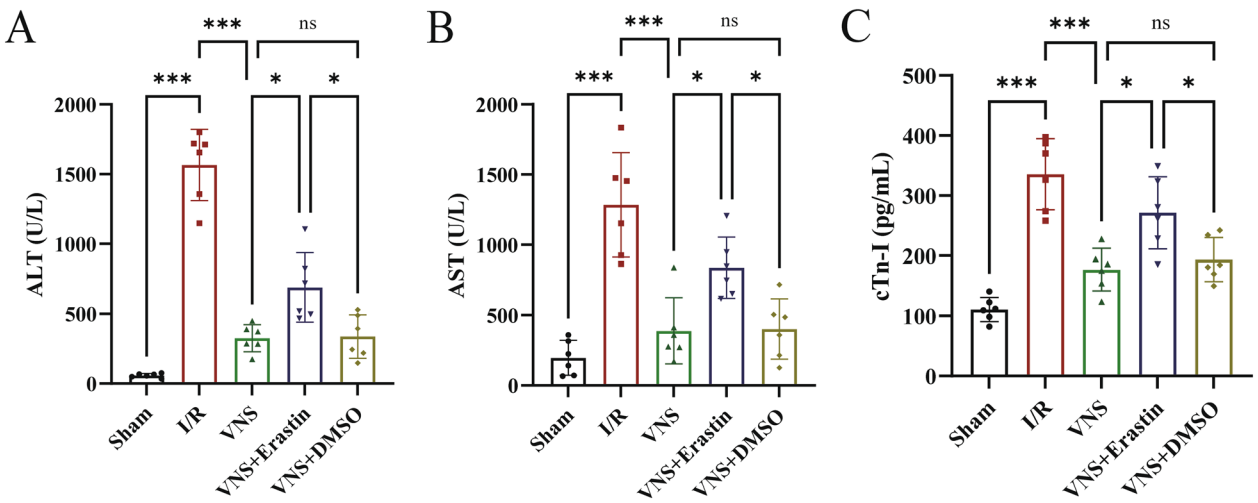

Fig.2 Changes in serum liver injury markers and myocardial injury markers after hepatic ischemia–reperfusion injury. **A** Serum levels of ALT in each group. **B** Serum levels of AST in each group. **C** Serum levels of cTnI in each group. ****P < 0.001, **P < 0.01, *P < 0.05, ns P > 0.05*

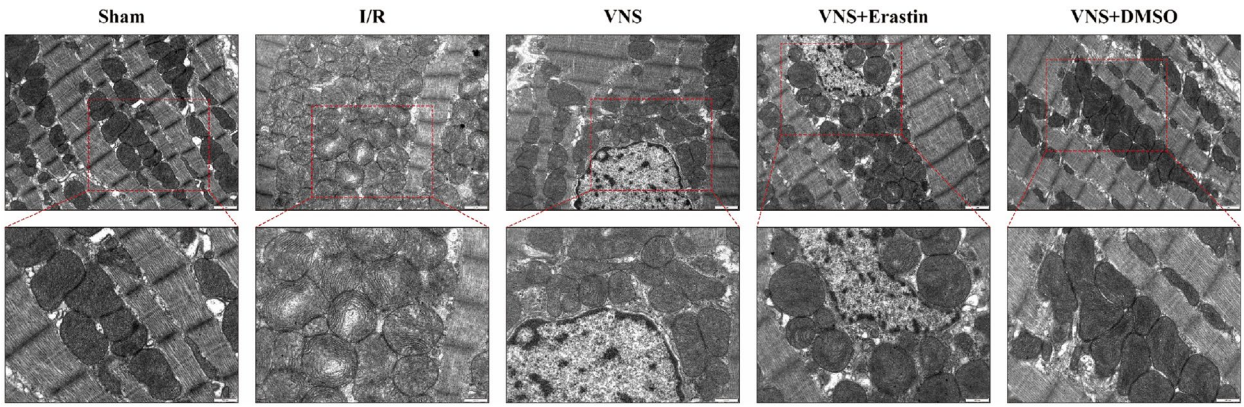

Fig.3 The effect of vagus nerve stimulation on mitochondrial damage in cardiomyocytes induced by hepatic ischemia–reperfusion injury. Representative transmission electron microscopy images of mitochondria structure

significantly increased compared to the Sham group ($P < 0.001$), thereby confirming the successful establishment of the hepatic I/R model. In the VNS group, serum ALT and AST levels were significantly reduced compared to the I/R group ($P < 0.001$) (Fig. 2A, B). Similarly, at 6 h after reperfusion, serum cTnI levels in the I/R group were significantly higher than in the Sham group ($P < 0.001$). In contrast, the VNS group showed significantly lower serum cTnI levels compared to the I/R group ($P < 0.001$) (Fig. 2C). To explore whether ferroptosis was involved in cardiac protection, erastin was intraperitoneally injected into rats with hepatic ischemia–reperfusion injury, alongside the treatment with VNS. The results showed that serum levels of ALT, AST, and cTnI in the VNS + Erastin group were significantly increased compared to the VNS group ($P < 0.05$) (Fig. 2A, C). Based on these findings, VNS demonstrates protective effects against hepatic I/R injury and the resulting myocardial injury, while erastin can negate the cardioprotective effects of VNS in this context.

VNS protects against mitochondrial damage in cardiomyocytes induced by hepatic I/R injury

Additionally, we utilized transmission electron microscopy to observe the morphological changes of mitochondria in cardiomyocytes and further investigated the protective effect of VNS on ferroptosis in cardiomyocytes induced by hepatic ischemia–reperfusion injury (Fig. 3). The results showed that the mitochondria in cardiomyocytes from the Sham group exhibited normal structure, with only slight swelling observed. In contrast, hepatic ischemia–reperfusion caused extensive swelling of mitochondria in myocardial tissue, leading to vacuolation, rupture and degradation of mitochondrial cristae

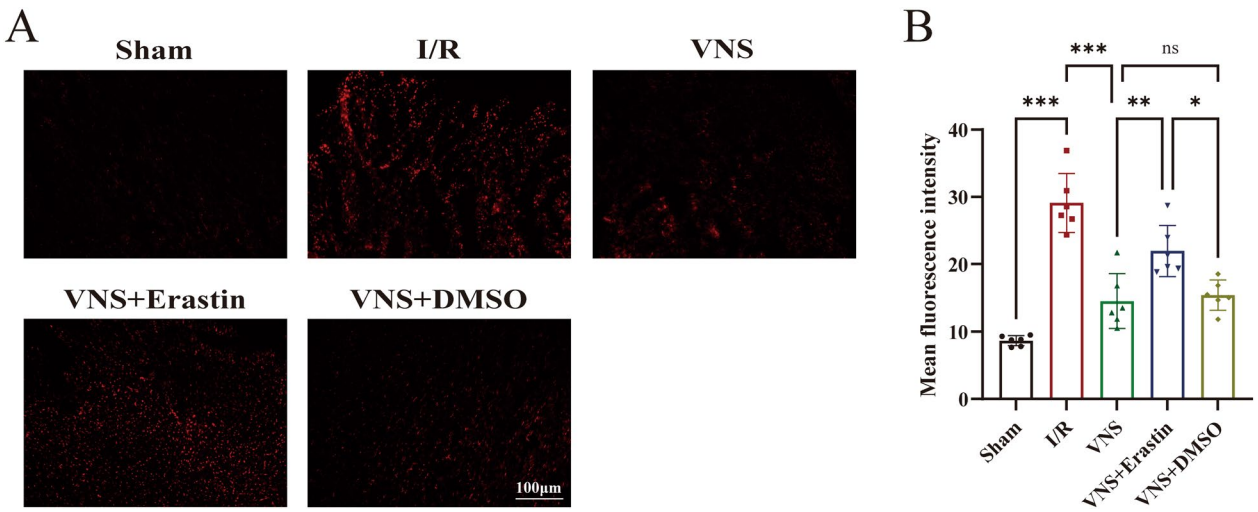

Fig.4 The effect of vagus nerve stimulation on the ROS levels in myocardium of rats with hepatic ischemia–reperfusion injury. **A** Representative fluorescent images of ROS, magnification 200. Scale bar, 100 μM. **B** Mean fluorescence intensity of ROS. ****P < 0.001, **P < 0.01, *P < 0.05, ns P > 0.05*

structures, and degradation of mitochondrial matrix, alongside an increased mitochondrial membrane density. Notably, the VNS group exhibited marked improvements over the I/R group, including reduced mitochondrial swelling and cristae degradation, disappearance of vacuolation, and restored mitochondrial membrane density. In addition, compared to the VNS group, the VNS + Erastin group showed further mitochondrial damage, with a significant number of mitochondrial cristae structures breaking and degrading, mitochondrial matrix degradation, mitochondrial swelling, the appearance of vacuolar lesions, and increased outer membrane density. indicating that erastin can counteract the protective effect of VNS. Conversely, compared to the VNS + Erastin group, the VNS + DMSO group showed substantial recovery in cristae structure, without obvious mitochondria swelling and matrix degradation. These results indicate that VNS can effectively improve the mitochondrial morphological changes and mitigate mitochondrial damage in cardiomyocytes induced by hepatic ischemia–reperfusion injury, while erastin can counteract this protective effect. However, DMSO does not affect the protective effect of VNS.

VNS reduces the levels of ROS in myocardium induced by hepatic I/R injury in rats

As indicated by ROS fluorescence staining analysis, only partial red fluorescence was observed in the myocardial tissue of the Sham group, indicating lower ROS levels. The I/R group exhibited a significant increase in red fluorescence, reflecting a marked elevation in ROS levels compared to the Sham group ($P < 0.001$). These results demonstrate that hepatic I/R exacerbates oxidative stress in myocardial tissue. Notably, compared to the I/R group, the VNS group showed reduced ROS generation ($P < 0.001$), confirming the inhibitory effect of VNS on oxidative stress. However, the VNS + Erastin group exhibited a significant increase in red fluorescence and elevated ROS levels compared to the VNS group ($P < 0.01$). In contrast, compared to the VNS + Erastin group, the VNS + DMSO group showed reduced red fluorescence and lower ROS levels ($P < 0.05$) (Fig. 4A, B). This finding suggests that erastin counteracts the inhibitory effect of VNS on oxidative stress by activating the ferroptosis process, while DMSO does not affect the role of VNS.

VNS alleviates iron overload and lipid peroxidation in myocardium induced by hepatic I/R injury in rats

Iron overload and lipid peroxidation are critical factors in the induction of ferroptosis [28]. To assess the effects of VNS on iron overload and lipid peroxidation in cardiomyocytes after hepatic I/R injury, we measured levels of Fe^{2+}, MDA, and GSH, along with SOD activity (Fig. 5). The I/R group exhibited significantly higher levels of Fe^{2+} and MDA compared to the Sham group ($P < 0.001$) (Fig. 5A, B), while GSH levels and SOD activity were significantly lower ($P < 0.001$) (Fig. 5C, D). These results indicate that hepatic I/R induces iron overload and lipid peroxidation in cardiomyocytes, accelerating the process of ferroptosis in cardiomyocytes. However, VNS significantly reversed these changes during the hepatic I/R process ($P < 0.001$), further confirming its cardioprotective effect. However, the VNS + Erastin group displayed lower GSH levels and SOD activity, along with higher Fe^{2+} and MDA

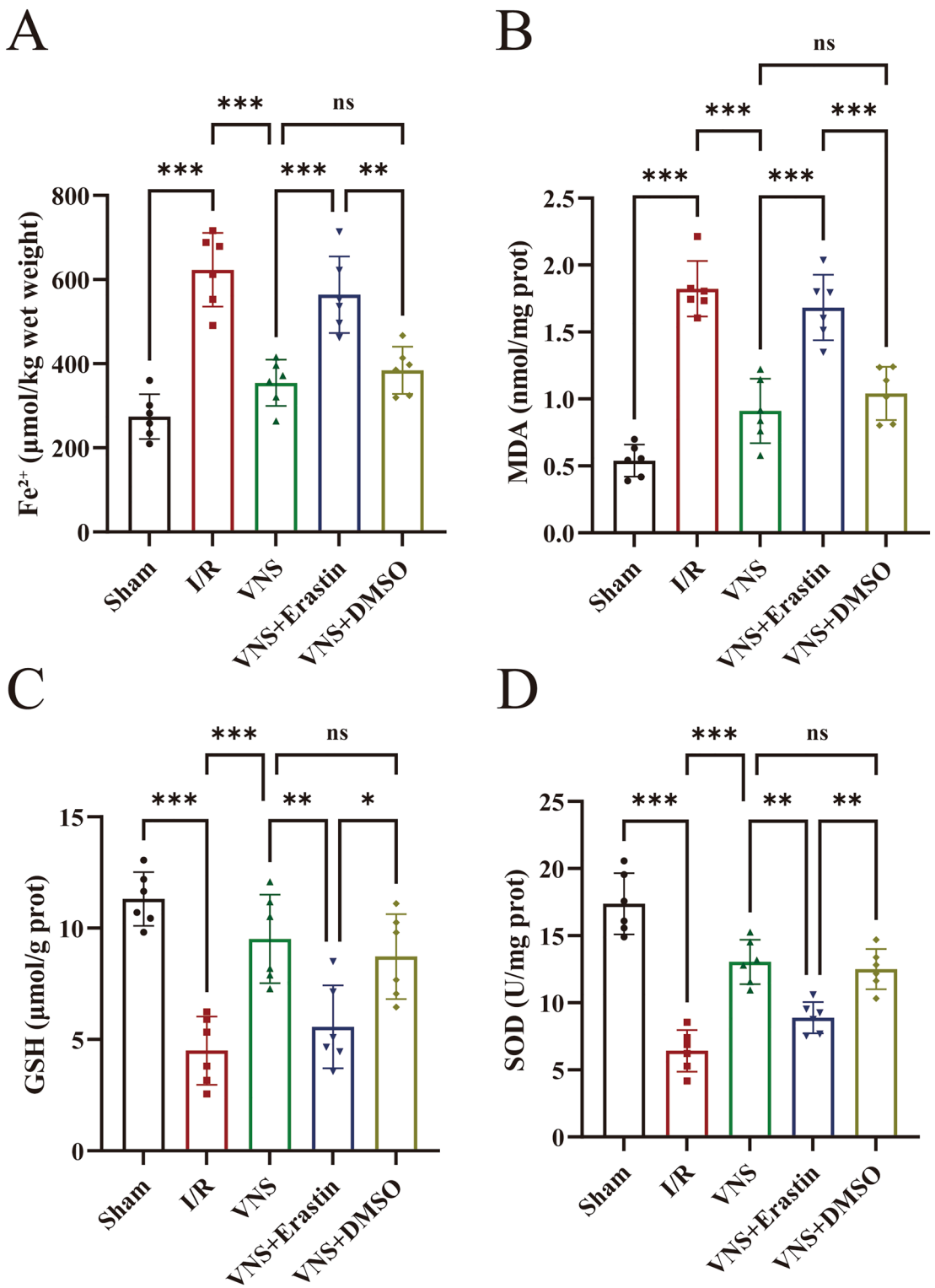

Fig.5 The effect of vagus nerve stimulation on iron overload and lipid peroxidation in myocardium of rats with hepatic ischemia–reperfusion injury. **A** The levels of Fe^{2+} in each group. **B** The content of MDA in each group. **C** The levels of GSH in each group. **D** The activity of SOD in each group. ****P < 0.001, **P < 0.01, *P < 0.05, ns P > 0.05*

levels compared to the I/R group ($P < 0.01$). Compared to the VNS + Erastin group, the VNS + DMSO group showed higher GSH levels and SOD activity and lower levels of Fe^{2+} and MDA ($P < 0.05$). Combined, these findings indicate that VNS alleviated ferroptosis in the myocardium following hepatic I/R injury, whereas the activation of ferroptosis counteracted the cardioprotective effects of VNS.

VNS significantly activates the SLC7A11/GPX4 axis in myocardial after hepatic I/R injury

To investigate whether the protective effect of VNS on myocardial injury resulting from hepatic I/R injury is mediated through the SLC7A11/GPX4 axis, we determined the expression levels of SLC7A11 and GPX4 in myocardial tissue using Western blot. Our results revealed that the expression levels of SLC7A11 and GPX4 were significantly downregulated in the I/R group compared to the Sham group ($P < 0.001$). However, VNS treatment effectively reversed the decrease in SLC7A11 ($P < 0.001$; Fig. 6A, B) and GPX4 ($P < 0.05$; Fig. 6C, D) expression in myocardial tissue caused by hepatic I/R injury. To further verify the role of ferroptosis and related pathways in VNS-mediated cardioprotection, we administered erastin (an SLC7A11 inhibitor). In comparison to the VNS group, erastin significantly downregulated the expression of SLC7A11 ($P < 0.001$) and further decreased GPX4 levels ($P < 0.05$) in rat myocardial tissue. These results indicate that the SLC7A11/GPX4 axis plays a vital role in VNS-induced cardioprotection by inhibiting ferroptosis.

Discussion

The primary finding of this study is that hepatic I/R injury can induces ferroptosis in cardiomyocytes, resulting in myocardial injury. In contrast, VNS provides a protective effect against liver and myocardial tissue damage in hepatic I/R rats. Notably, VNS has been found for the first time to primarily reduce oxidative stress, alleviate mitochondrial damage, and prevent ferroptosis by activating the SLC7A11/GPX4 axis, thereby preventing myocardial injury caused by hepatic I/R.

During hepatic I/R, ischemia leads to the production of substantial amounts of ROS in the liver, which are inadequately cleared. Upon reperfusion, these ROS are released in large quantities, triggering a series of pathophysiological responses, including lipid peroxidation and biomembrane damage, and inflammatory responses, all of which worsen tissue injury [5]. The heart, in particular, is highly vulnerable to ROS-mediated damage during hepatic I/R. Our findings indicated that hepatic I/R significantly increased serum levels of ALT, AST, and cTnI in rats. The result is consistent with previous research [5], further confirming that hepatic I/R injury can cause myocardial injury. Moreover, existing literature has demonstrated that the vagus nerve exerts protective effects against myocardial ischemia–reperfusion injury [20]. Our data showed that VNS can reduce the elevated serum levels of ALT, AST, and cTnI in rats with hepatic ischemia–reperfusion injury. The result indicates that VNS can reduce hepatic ischemia–reperfusion injury and the resulting myocardial damage.

Oxidative stress is a vital factor in myocardial injury. Research has shown that it can mediate myocardial injury by inducing cardiomyocyte death [29]. Ferroptosis, a form of iron-dependent cell death driven by lipid peroxidation, is intimately associated with oxidative stress, especially during reperfusion [10]. The heart is especially vulnerable to damage from iron overload [11]. Additionally, studies have shown that hepatic I/R injury can induce oxidative stress responses in distal myocardium [30]. Therefore, we speculated that hepatic I/R may induce ferroptosis in cardiomyocytes. Previous studies have demonstrated that VNS can exhibit cardioprotective effects, capable of mitigating drug-induced cardiotoxicity from agents such as doxorubicin and trastuzumab by inhibiting ferroptosis [31, 32]. Therefore, we hypothesized that VNS might protect against myocardial injury resulting from hepatic I/R injury by inhibiting ferroptosis. GSH is an important hydrophilic antioxidant that scavenges ROS, serving as the first line of antioxidant defense during reperfusion [33]. Additionally, SOD plays a vital role by catalyzing the dismutation of ROS, thereby reducing its toxicity. These changes indicate that VNS enhances the ability of myocardial tissue to eliminate excess ROS. Furthermore, we observed that VNS significantly reduced elevated levels of iron, ROS, and MDA in the myocardial tissue of rats subjected to hepatic I/R, alleviating mitochondrial damage. These results supported our hypothesis that cardiomyocytes experience iron overload and lipid peroxidation during hepatic I/R, while VNS can alleviate this phenomenon to some extent, thereby reducing the occurrence of ferroptosis. Notably, although iron levels in cardiomyocytes from the VNS group remained higher than in those from the Sham group, VNS could alleviate myocardial injury caused by hepatic I/R to some extent through the inhibition of ferroptosis.

Further research indicated that VNS mitigates ferroptosis in cardiomyocytes due to hepatic I/R by enhancing the SLC7A11/GPX4 axis, a crucial defense mechanism against ferroptosis. Specifically, GPX4, utilizing glutathione as a cofactor, converts lipid peroxides into nontoxic lipid alcohols, thus preventing the accumulation of toxic lipid ROS and maintaining intracellular lipid homeostasis [34]. The reduction of GPX4 activity is positively correlated with the increase of oxidative stress and cell

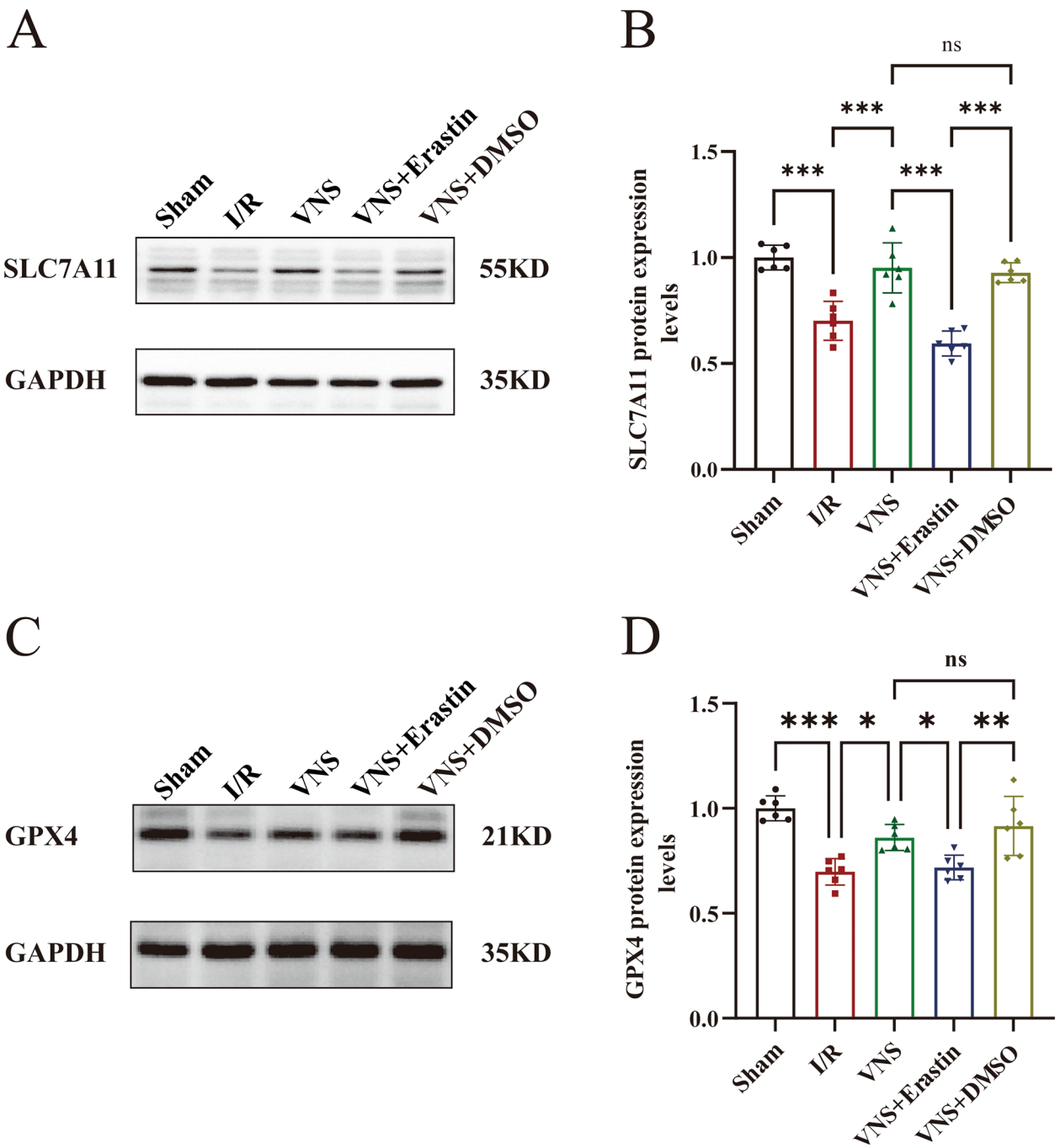

Fig.6 The effect of vagus nerve stimulation on the SLC7A11/GPX4 axis on the myocardium of rats with hepatic ischemia–reperfusion injury. **A** Representative western blot bands of SLC7A11 in each group. **B** Relative protein expression of SLC7A11 in each group. **C** Representative western blot bands of GPX4 in each group. **D** The level of expression of GPX4 in each group. ****P < 0.001, **P < 0.01, *P < 0.05, ns P > 0.05*

death across various diseases [35]. The SLC7A11/GPX4 axis is critical for GSH synthesis, maintaining cellular redox homeostasis, and inhibiting ferroptosis. Notably, the upregulation of SLC7A11 increased the expression of GPX4, further suppressing ferroptosis [36]. In this study, we found that VNS significantly mitigates GSH depletion in the myocardium of rats with hepatic I/R and increases the protein expressions of SLC7A11 and GPX4. These findings indicated that VNS exerts cardioprotective effects by enhancing the SLC7A11/GPX4 axis.

Prior research has demonstrated that VNS can inhibit the recruitment of inflammatory cells and the release of cytokines through the cholinergic anti-inflammatory pathway, reducing myocardial ischemia–reperfusion injury [37]. Our findings further confirmed the protective effect of VNS on cardiac injury caused by hepatic I/R and revealed one of its possible mechanisms, namely the regulation of the SLC7A11/GPX4 ferroptosis pathway. This important finding not only enriches our understanding of the mechanisms by which VNS protects distant organs (especially the heart) from damage during hepatic ischemia–reperfusion, but also opens up highly promising new targets for the development of novel myocardial protection strategies.

To further elucidate the mechanism by which VNS improves myocardial injury caused by hepatic I/R, we utilized the xCT inhibitor erastin as an additional intervention. Erastin inhibits the SLC7A11 subunit to block the uptake of cysteine through the system xc−, which leads to GSH depletion and GPX4 inactivation, ultimately inducing ferroptosis [38]. Our results showed that erastin negated the therapeutic effects of VNS, further confirming that VNS mitigates ferroptosis and exerts cardioprotective effects through the activation of the SLC7A11/GPX4 axis. Prior studies have demonstrated that VNS exerts cardioprotective effects by regulating the AMP-activated protein kinase (AMPK) signaling pathway [39]. Additionally, Nrf2, a negative regulator of ferroptosis, has been shown to upregulate downstream antioxidants within AMPK-mediated antioxidative responses [40]. GPX4 and SLC7A11 are transcriptional targets of Nrf2 [41]. VNS has been found to activate the Nrf2/HO-1 pathway [19]. Therefore, we hypothesized that VNS may regulate the SLC7A11/GPX4 axis by activating the AMPK pathway, thereby alleviating myocardial injury resulting from hepatic ischemia–reperfusion injury. However, the precise mechanism by which VNS modulates the SLC7A11/GPX4 axis via the AMPK pathway in this context remains unclear. Our future research will further explore this mechanism, aiming to clarify how VNS regulates these molecules to exert its cardioprotective effects. Our findings contribute to more comprehensively understand the cardioprotective mechanism of VNS and provide a more solid theoretical foundation for its clinical application.

However, this study has several limitations that should be considered in future research. First, the reperfusion time after hepatic ischemia in this study is only 6 h, which is in the early stage of I/R. During this period, damage primarily stems from ROS produced by Kupffer cells. However, after 6 h of reperfusion, the recruitment of neutrophils and the release of oxidants and proteases complicate the injury response, potentially influencing the therapeutic effect of VNS. Therefore, future studies should extend the reperfusion duration to more comprehensively evaluate the therapeutic effect of VNS across different stages of hepatic I/R. Finally, varying frequencies, intensities, and durations of VNS may yield different therapeutic effects. However, this study only used a single set of stimulation parameters. Therefore, future research should explore the impact of different VNS parameters on therapeutic outcomes to optimize VNS treatment protocols.

Conclusions

In conclusion, our findings demonstrate that VNS alleviates myocardial injury by reducing oxidative stress, mitochondrial damage, and ferroptosis in cardiomyocytes resulting from hepatic I/R injury. This protective effect is mediated by the activation of the SLC7A11/GPX4 axis. These findings provide new theoretical and experimental support for the application of VNS in the field of myocardial protection during clinical liver surgeries and transplants, and offer new insights into the role of ferroptosis in myocardial injury.

Abbreviations

VNS	Vagus nerve stimulation
I/R	Ischemia–reperfusion
ALT	Alanine aminotransferase
AST	Aspartate aminotransferase
cTnI	Cardiac troponin I
ROS	Reactive oxygen species
MDA	Malondialdehyde
SOD	Superoxide dismutase
GSH	Glutathione
GPX4	Glutathione peroxidase-4
xCT	Cystine-glutamate antiporter system
PUFAs	Polyunsaturated fatty acids
AMPK	AMP-activated protein kinase

Supplementary Information

The online version contains supplementary material available at https://doi.org/10.1186/s40001-025-02416-7.

Supplementary Material 1.

Acknowledgements

We sincerely thank the Anesthesia Laboratory of the Second Hospital of Shanxi Medical University for their valuable support and assistance.

Author contributions

Po Zhang and Yuanjing Qin designed the research. Po Zhang, Yuanjing Qin, and Haiyan Wang conducted the experiments and acquired the data. They were also responsible for data analysis. Po Zhang, Yuanjing Qin, and Jinping Wang wrote the original draft. Jinping Wang participated in the editing process, provided feedback on the manuscript, oversaw the project, guided other researchers, and secured financial support for the research. All the authors have contributed to the completion of this paper.

Funding
This study was supported by Shanxi Provincial Health Commission "Four batch" Science and technology medical innovation plan (Grant No.2023XM023) and Jincheng Science and Technology Bureau Key R&D Plan (Social Development field) (Grant No.20220206).

Availability of data and materials
No datasets were generated or analysed during the current study.

Declarations

Ethics approval and consent to participate
The study was approved by the Ethics Committee of the Second Hospital of Shanxi Medical University (DW2024028).

Consent for publication
All authors consented for the publication.

Competing interests
The authors declare no competing interests.

Author details
[1]College of Anesthesiology, Shanxi Medical University, 86 Xinjiannan Road, Taiyuan 030001, Shanxi, China. [2]Department of Anesthesiology, Jincheng People's Hospital, 1666 Baishui East Street, Jincheng 048026, Shanxi, China.

Received: 12 December 2024 Accepted: 27 February 2025
Published online: 12 March 2025

References

1. Jimenez-Castro MB, Cornide-Petronio ME, Gracia-Sancho J, Peralta C. Inflammasome-mediated inflammation in liver ischemia-reperfusion injury. Cells. 2019. https://doi.org/10.3390/cells8101131.
2. Lin X, et al. A bibliometric and visualized analysis of hepatic ischemia-reperfusion injury (HIRI) from 2002 to 2021. Heliyon. 2023;911: e22644.
3. Mouratidou C, et al. Hepatic ischemia-reperfusion syndrome and its effect on the cardiovascular system: the role of treprostinil, a synthetic prostacyclin analog. World J Gastrointest Surg. 2023;159:1858–70.
4. Cannistra M, et al. Hepatic ischemia reperfusion injury: a systematic review of literature and the role of current drugs and biomarkers. Int J Surg. 2016;33(Suppl 1):S57-70.
5. An W, Kang JS. Effect of metformin on myocardial injury induced by hepatic ischemia-reperfusion in rats. Front Pharmacol. 2022;13: 822743.
6. Nastos C, et al. Global consequences of liver ischemia/reperfusion injury. Oxid Med Cell Longev. 2014;2014: 906965.
7. Lambert EA, et al. Sympathetic nervous response to ischemia-reperfusion injury in humans is altered with remote ischemic preconditioning. Am J Physiol Heart Circ Physiol. 2016;3112:H364-370.
8. Wu X, Li Y, Zhang S, Zhou X. Ferroptosis as a novel therapeutic target for cardiovascular disease. Theranostics. 2021;117:3052–9.
9. Baba Y, et al. Protective effects of the mechanistic target of rapamycin against excess iron and ferroptosis in cardiomyocytes. Am J Physiol Heart Circ Physiol. 2018;3143:H659–68.
10. Luo L, Mo G, Huang D. Ferroptosis in hepatic ischemia-reperfusion injury: regulatory mechanisms and new methods for therapy (review). Mol Med Rep. 2021. https://doi.org/10.3892/mmr.2021.11864.
11. Guo L, et al. Yiqifumai injection ameliorated sepsis-induced cardiomyopathy by inhibition of ferroptosis Via Xct/Gpx4 axis. Shock. 2024;614:638–45.
12. Zhao WK, Zhou Y, Xu TT, Wu Q. Ferroptosis: opportunities and challenges in myocardial ischemia-reperfusion injury. Oxid Med Cell Longev. 2021;2021:9929687.
13. Wang L, et al. Transcutaneous auricular vagus nerve stimulators: a review of past, present, and future devices. Expert Rev Med Devices. 2022;191:43–61.
14. Hilz MJ. Transcutaneous vagus nerve stimulation—a brief introduction and overview. Auton Neurosci. 2022;243: 103038.
15. Yuan H, Silberstein SD. Vagus nerve and Vagus nerve stimulation, a comprehensive review: part III. Headache. 2016;563:479–90.
16. Wang M, et al. Vagus nerve stimulation ameliorates renal ischemia-reperfusion injury through inhibiting NF-kappaB activation and iNOS protein expression. Oxid Med Cell Longev. 2020;2020:7106525.
17. Tang H, et al. Vagus nerve stimulation alleviated cerebral ischemia and reperfusion injury in rats by inhibiting pyroptosis via alpha7 nicotinic acetylcholine receptor. Cell Death Discov. 2022;81:54.
18. Zhao JJ, et al. The mechanisms through which auricular vagus nerve stimulation protects against cerebral ischemia/reperfusion injury. Neural Regen Res. 2022;173:594–600.
19. Zhang Q, et al. Vagus nerve stimulation attenuates hepatic ischemia/reperfusion injury via the Nrf2/HO-1 pathway. Oxid Med Cell Longev. 2019;2019:9549506.
20. Nuntaphum W, et al. Vagus nerve stimulation exerts cardioprotection against myocardial ischemia/reperfusion injury predominantly through its efferent vagal fibers. Basic Res Cardiol. 2018;1134:22.
21. Deng S, Zhang Y, Xin Y, Hu X. Vagus nerve stimulation attenuates acute kidney injury induced by hepatic ischemia/reperfusion injury in rats. Sci Rep. 2022;121:21662.
22. Xin Y, Zhang Y, Deng S, Hu X. Vagus nerve stimulation attenuates acute skeletal muscle injury induced by hepatic ischemia/reperfusion injury in rats. Front Pharmacol. 2021;12: 756997.
23. Xu YP, et al. The protective effect of vagus nerve stimulation against myocardial ischemia/reperfusion injury: pooled review from preclinical studies. Front Pharmacol. 2023;14:1270787.
24. Chen M, et al. Hype or hope: Vagus nerve stimulation against acute myocardial ischemia-reperfusion injury. Trend Cardiovasc Med. 2020;308:481–8.
25. Hausenloy DJ, et al. Cardiac innervation in acute myocardial ischaemia/reperfusion injury and cardioprotection. Cardiovasc Res. 2019;1157:1167–77.
26. Mei SL, et al. Shenmai injection attenuates myocardial ischemia/reperfusion injury by targeting Nrf2/GPX4 signalling-mediated ferroptosis. Chin J Integr Med. 2022;2811:983–91.
27. Ramani R. Vagus nerve stimulation therapy for seizures. J Neurosurg Anesthesiol. 2008;201:29–35.
28. Liu H, et al. Rhein attenuates cerebral ischemia-reperfusion injury via inhibition of ferroptosis through NRF2/SLC7A11/GPX4 pathway. Exp Neurol. 2023;369: 114541.
29. Park TJ, et al. Quantitative proteomic analyses reveal that GPX4 downregulation during myocardial infarction contributes to ferroptosis in cardiomyocytes. Cell Death Dis. 2019;1011:835.
30. Chen CF, et al. Ischemia/reperfusion of the liver induces heart injury in rats. Transplant Proc. 2007;394:855–7.
31. Prathumsap N, et al. Vagus nerve stimulation exerts cardioprotection against doxorubicin-induced cardiotoxicity through inhibition of programmed cell death pathways. Cell Mol Life Sci. 2022;801:21.
32. Prathumsap N, et al. Muscarinic and nicotinic receptors stimulation by vagus nerve stimulation ameliorates trastuzumab-induced cardiotoxicity via reducing programmed cell death in rats. Toxicol Appl Pharmacol. 2024;491: 117074.
33. Haramaki N, et al. Networking antioxidants in the isolated rat heart are selectively depleted by ischemia-reperfusion. Free Radic Biol Med. 1998;253:329–39.
34. Forcina GC, Dixon SJ. GPX4 at the crossroads of lipid homeostasis and ferroptosis. Proteomics. 2019;1918: e1800311.
35. Zhang W, et al. GPX4, ferroptosis, and diseases. Biomed Pharmacother. 2024;174: 116512.
36. Yu P, et al. Dexmedetomidine post-conditioning alleviates myocardial ischemia-reperfusion injury in rats by ferroptosis inhibition via SLC7A11/GPX4 axis activation. Hum Cell. 2022;353:836–48.
37. Zhao M, et al. Vagal stimulation triggers peripheral vascular protection through the cholinergic anti-inflammatory pathway in a rat model of myocardial ischemia/reperfusion. Basic Res Cardiol. 2013;1083:345.
38. Chen B, Fan P, Song X, Duan M. The role and possible mechanism of the ferroptosis-related SLC7A11/GSH/GPX4 pathway in myocardial ischemia-reperfusion injury. BMC Cardiovasc Disord. 2024;241:531.
39. Xue RQ, et al. Vagal nerve stimulation improves mitochondrial dynamics via an M(3) receptor/CaMKKbeta/AMPK pathway in isoproterenol-induced myocardial ischaemia. J Cell Mol Med. 2017;211:58–71.

40. Wang X, et al. Ferroptosis is essential for diabetic cardiomyopathy and is prevented by sulforaphane via AMPK/NRF2 pathways. Acta Pharm Sin B. 2022;122:708–22.
41. Sedlackova L, Korolchuk VI. Mitochondrial quality control as a key determinant of cell survival. Bba-Mol Cell Res. 2019;18664:575–87.

Publisher's Note